

# A Raman Study of Morphotropic Phase Boundary in $\text{PbZr}_{1-x}\text{Ti}_x\text{O}_3$ at low temperatures

K. C. V. Lima, A. G. Souza \*, A. P. Ayala, J. Mendes Filho,  
P. T. C. Freire, and F. E. A. Melo

*Departamento de Física, Universidade Federal do Ceará, Caixa Postal 6030,  
Campus do Pici, 60455-760 Fortaleza, Ceará, Brazil*

E. B. Araújo and J. A. Eiras

*Departamento de Física, Universidade Federal de São Carlos, Caixa Postal 676,  
13565-670 São Carlos SP - Brazil*

(October 25, 2018)

Raman spectra of  $\text{PbZr}_{1-x}\text{Ti}_x\text{O}_3$  ceramics with titanium concentration varying between 0.40 and 0.60 were measured at 7 K. By observing the concentration-frequency dependence of vibrational modes, we identified the boundaries among rhombohedral, monoclinic, and tetragonal ferroelectric phases. The analysis of the spectra was made in the view of theory group analysis making possible the assignment of some modes for the monoclinic phase.

Pacs number: 77.84.Dy, 77.84.-s, 77.80.Bh

## I. INTRODUCTION

The  $\text{PbZr}_{1-x}\text{Ti}_x\text{O}_3$  (PZT) solid-solution system contains several compositions that are suited to important technological applications in the electronic field such as piezoelectric transducers, pyroelectric detectors, and non-volatile ferroelectric memories. The main applications of PZT have been as transducers that are fabricated using compositions closely related to the Morphotropic Phase Boundary (MPB)<sup>1</sup>. For this reason, MPB has been widely investigated from both experimental techniques<sup>2</sup> and theoretical approaches<sup>3</sup>. In this region, PZT exhibits outstanding electromechanical properties which have been attributed to the compositional fluctuations being they treated within the framework of a phase coexistence theory<sup>4</sup>. Following this, a detailed nature of physical properties for compositions close to MPB was not well established.

The recent discovery of a new monoclinic ferroelectric phase by Noheda et al.<sup>5</sup> has shed a new light on the understanding of the dielectric and piezoelectric enhancement for compositions in the vicinity of MPB. In fact, the monoclinic distortion was interpreted as either a condensation along one of the (110) directions of the local displacements present in the tetragonal phase,<sup>6</sup> or as a condensation along one of the (100) directions of the local displacements present in the rhombohedral phase.<sup>7</sup> This monoclinic phase exhibited by PZT at low temperatures would be the first example of a ferroelectric material with  $P_x^2 = P_y^2 \neq P_z^2$ , where  $P_x^2, P_y^2, P_z^2 \neq 0$ .<sup>5</sup> Hence, the monoclinic structure can be considered as a derivative form from both tetragonal and rhombohedral phases by representing a link between them. This model provides a microscopic picture where such a striking electromechanical response close to the MPB region<sup>6</sup> is associated with the monoclinic distortion. A successful explanation for the large piezoelectricity found in PZT ceramics near the MPB was recently obtained by means of first-principle calculations<sup>8</sup>. The piezoelectric coefficients

were calculated by considering the rotation of the polarization vector in the monoclinic plane that is the unique characteristic of monoclinic phase when compared with all other ferroelectrics<sup>8</sup>. Also, the stability of the monoclinic phase was recently described by means of phenomenological thermodynamic studies within the framework of Landau-Devonshire theory<sup>9</sup> by considering the linear coupling between the polarization and the monoclinic distortion  $\beta-90^\circ$ .

In spite of all investigations of the monoclinic phase in PZT system, Raman studies performed on this new phase<sup>9,10</sup> were limited to only two Ti concentration. However, information on the phase transitions for other PZT compositions close to the MPB is strongly desirable and appears as an interesting investigation. In this way, the purpose of this work is to investigate the extension of monoclinic phase for compositions close to the MPB through Raman spectroscopy at low temperatures. A careful analysis of the data allowed us to determine the extension of monoclinic phase based on the phonon behavior at low temperatures.

## II. EXPERIMENTAL

Samples of  $\text{PbZr}_{1-x}\text{Ti}_x\text{O}_3$  (with  $0.40 \leq x \leq 0.52$ ) were obtained through the solid-state reaction from 99.9 % pure reagent grade  $\text{PbO}$ ,  $\text{ZrO}_2$  and  $\text{TiO}_2$  oxides. The starting powders and distilled water were mixed and milled during 3.5 hours for powder homogenization. The mixture was calcined at  $850^\circ\text{C}$  for 2.5 h. It was pressed at 400 MPa giving rise to PZT ceramics disks with 10 mm of diameter and 5 mm of thickness. Finally, the disks were sintered at temperature of  $1250^\circ\text{C}$  during 4h and an excellent ceramics homogeneity was obtained. The sintering atmosphere, which consists of a covered alumina crucible, was enriched in  $\text{PbO}$  vapor using  $\text{PbZrO}_3$  powder around the disks in order to avoid significant volatilization of  $\text{PbO}$ .

MicroRaman measurements were performed using a T64000 Jobin Yvon Spectrometer equipped with an Olympus microscope and a N<sub>2</sub>-cooled CCD to detect scattered light. The spectra were excited with an Argon ion Laser ( $\lambda = 514.5$  nm). The spectrometer slits were set to give a spectral resolution of better than  $2$  cm<sup>-1</sup>. A Nikon 20x objective with focal distance 20 mm and numeric aperture N.A. = 0.35 was employed to focus the laser beam on the polished sample surface. Low temperature measurements were performed using an Air Products closed-cycle refrigerator which provides temperatures ranging from 7 to 300 K. A Lakeshore controller was used to control the temperature with precision of order of  $\pm 0.1$  K.

We have made a systematic study of the laser-induced heating on the samples in order to estimate the temperature through the Stokes/anti-Stokes ratio and improve a better signal/noise ratio. The samples close to the MPB present a strong elastic scattering which leads to a calculation of temperature by means of the Stokes/anti-Stokes ratio not reliable. Then, we used a PbZr<sub>0.98</sub>Ti<sub>0.02</sub>O<sub>3</sub> sample whose spectra can be easily fitted and the temperature estimate was reproducible. Following our observations we used a laser power of order of 0.1 mW.

### III. RESULT AND DISCUSSION

In Fig. 1, Raman spectra for several PZT compositions varying from 0.40 to 0.60 are displayed. From  $x = 0.40$  to  $x = 0.46$ , the spectra remain exactly the same or change slightly, not only in frequency but also in relative intensity for all modes. At 7 K, it is expected a phase transition from rhombohedral low temperature ( $R_{LT}$ ) to rhombohedral high temperature ( $R_{HT}$ ) phase. The boundary between  $R_{LT}$  and  $R_{HT}$  has been established by Jaffe et al<sup>1</sup> for temperatures higher than 300 K. An extension of this boundary to low temperatures was made by Amin et al<sup>13</sup> for composition  $x=0.40$ , and more recently by Noheda et al<sup>12</sup> for  $x=0.42$ .

The  $R_{LT}$  phase, whose space group is  $C_{3v}^6$ , is characterized by opposite rotations of adjacent oxygen octahedra along the [111] polar axis. Due to this fact, the unit cell of  $R_{LT}$  phase has a volume twice the unit cell of  $R_{HT}$  whose space group is  $C_{3v}^5$ . From the diffraction point of view, this transition is detected through the appearance of very weak superlattice peaks which are originated just from the doubling of the unit cell<sup>13</sup>. Concerned with the vibrational properties, the dispersion relation for  $R_{LT}$  phase is obtained by folding the dispersion curves of  $R_{HT}$  phase. Thus, the observation of additional Raman modes is expected since wave vectors belonging to the zone boundary have after the zone folding, pseudomomenta equivalent to  $q=0$ . For Zr-rich PZT, this phase transition was observed from Raman spectroscopy by analyzing the low frequency modes located at about 62 and 68 cm<sup>-1</sup> which are, according to El-Harrad et al<sup>14</sup>, ex-

clusive features of the  $R_{LT}$  and  $R_{HT}$  phase, respectively. The mode at 62 cm<sup>-1</sup> is initially a zone boundary mode that becomes a zone center active mode due to the doubling of the unit cell. In the vicinity of the MPB, this kind of analysis is somewhat complicated due to the overlapping of the bands which difficult the fitting procedure and the identification of phase transition. In the intermediate frequency region ( $120 \leq \omega \leq 400$  cm<sup>-1</sup>, shown in Fig. 1) significant changes are not expected in the vibrational modes since they are closely related to the intrinsic modes of octahedral units such as stretching, torsion, and bending.

Upon increasing Ti concentration, the spectra for 0.47 and 0.50 exhibits new features. Two of them are remarkable. First, the intensity of the mode located at about 240 cm<sup>-1</sup> (marked with a solid arrow) in rhombohedral phase decreases entering into background for concentrations higher than  $x = 0.48$ . Second, the mode at about 280 cm<sup>-1</sup> (marked with a dot arrow) for  $x=0.40$  presents a splitting resulting in a doublet mode. These spectral changes were interpreted as due to the rhombohedral - monoclinic phase transition. Thus, the boundary between  $R_{LT}$  and monoclinic structure is closely related to composition 0.46. Noheda et al<sup>12</sup> observed that PZT with  $x=0.46$  is in a monoclinic structure down to 20 K. Our results show that this composition is justly in the rhombohedral - monoclinic transition region. Since the boundary between  $R_{HT}$  and monoclinic structure is almost vertical, we believe that a small deviation in composition accounts for the observed disagreement between our results and those reported in Ref.<sup>12</sup>.

In the first analysis, there are no clear changes in the Raman spectra from  $x=0.48$  to  $x=0.60$ . However, the monoclinic-tetragonal phase transition is expected around  $x=0.52$ <sup>12</sup>. In order to study the effects of the phase transition in the phonon spectra we constructed the frequency versus  $x$  ( $\omega$  vs.  $x$ ) plot where the transitions can be observed in details. The frequencies were obtained by deconvoluting the spectra using a set of curves with lorentzian shapes. The number of peaks used to fit spectra were determined by means of group theory analysis that will be discussed in a forthcoming paragraph. In Fig. 2, we shown the deconvoluted spectrum for tetragonal PbZr<sub>0.60</sub>Ti<sub>0.40</sub>O<sub>3</sub> following the procedure and assignment earlier reported<sup>10</sup> where observed frequencies are in good agreement with those found there.

In order to understand the tetragonal - monoclinic transition, let us first discuss the mode symmetry related to tetragonal phase in PbTiO<sub>3</sub>. When the cubic phase transforms into tetragonal, the  $T_{2u}$  silent mode transforms into  $B_1 \oplus E$  irreducible representation of the  $C_{4v}$  and a degeneracy breaking of this mode is expected<sup>11</sup>. Besides its Raman activity in  $C_{4v}$  symmetry, this mode has been called a *silent* mode and its splitting was not observed for PbTiO<sub>3</sub> at room temperature<sup>11</sup>. However, when Ti is replaced by Zr, the splitting is observed at low temperatures. The member of the doublet with higher frequency is assigned as the  $B_1$  mode<sup>10</sup> and the value

$\omega_{B_1} - \omega_E$  increases in the vicinity of MPB. This observation was made by Frantti et al<sup>10</sup> who studied this feature from compositions  $x=0.49, 0.50, 0.60, 0.70, 0.80$  and  $0.90$ . Here, we extend this study inserting intermediate compositions making possible a detailed description of  $B_1$  mode when monoclinic - tetragonal transition take place. To describe the phase transition in details, we have constructed, based on the group theory analysis, the  $\omega$  vs.  $x$  plot shown in Fig. 3a. The point group of monoclinic phase is  $C_s$  where all the irreducible representation ( $A'$  and  $A''$ ) are Raman active. The  $C_s$  group is subgroup of both  $C_{3v}$  and  $C_{4v}$  and the correlation between them and  $O_h$  can be summarized in the scheme showed in Fig. 4. Following that scheme, we observe that  $B_1$  and  $E$  modes belonging to the tetragonal phase transforms into  $A''$  and  $A' \oplus A''$ , respectively. Therefore, we have used three modes in the monoclinic phase to fit the region around  $280 \text{ cm}^{-1}$ . It is interesting to note that highest frequency member of doublet  $A' \oplus A''$  presents the same behavior early reported by Frantti et al<sup>10</sup>.

We also plotted in Fig. 3b our results and those earlier reported<sup>10,11</sup> for several compositions in a small frequency region. In this figure we can observe that  $B_1$  mode decreases in frequency from  $x=1.0$  to  $x=0.60$  and increases from  $x=0.60$  to  $x=0.52$ . Below  $x=0.52$ , it decreases(increases) for Ti content from  $0.52$  to  $0.50$  ( $0.48$  to  $0.47$ ). The tetragonal - monoclinic phase transition can be observed by analyzing the splitting  $\Delta\omega$  ( $\omega_{B_1} - \omega_E$  in tetragonal phase and  $\omega_{A''}$ -the highest frequency member of  $A' \oplus A''$  in monoclinic phase). This splitting in the tetragonal phase ( $x \geq 0.52$ ) decreases when Ti content increases while it presents the same behavior exhibited by  $B_1$  mode in the monoclinic region (Fig. 3c). Both changes in  $B_1$  and in  $\Delta\omega$  indicate the transition between monoclinic and tetragonal symmetry. Noheda et al<sup>12</sup> reported that composition  $x=0.52$  presents a tetragonal symmetry at  $20 \text{ K}$ . Our results at  $7 \text{ K}$  indicate that this composition is in a monoclinic phase. In principle, our results do not differ from those of Ref.<sup>12</sup> and we believe that either a small deviation in  $x$  or the extension of monoclinic - tetragonal boundary can account for the minor disagreement between their and our results. For the sake of completeness, the frequencies of doublet mode depicted in Fig. 3b for several compositions are listed in Table I.

A similar analysis based on the group theory can be performed to describe the  $R_{HT}$  - monoclinic phase transition observed around  $x=0.46$ . When the cubic ( $O_h$ ) phase transforms into rhombohedral  $C_{3v}$  phase, the  $T_{2u}$  silent mode transforms into  $A_2 \oplus E$  irreducible representation being  $A_2$  without Raman activity. For this reason, there is a single peak at about  $280 \text{ cm}^{-1}$  for compositions with rhombohedral phase. By observing the correlation between the  $C_{3v}$  and  $C_s$  depicted in Fig. 4 we can observe the splitting of this mode into three new modes, i.e.,  $A' \oplus 2A''$  which are in a perfect accordance when we describe the transition from tetragonal side.

Let us now try to discuss the monoclinic phase based

on the assumptions of distortion of the unit cell by strain. The polar axis in the monoclinic phase has a particular feature if it is compared with that of tetragonal and rhombohedral phase. In fact, it can not be determined only by symmetry and can be along any direction within the monoclinic plane. This consideration was introduced by first-principle calculation made by Bellaiche et al<sup>8</sup> where the striking piezoelectric properties for monoclinic compositions were successfully obtained. To the best of our knowledge, there is no systematic theoretical study concerned with what happens with optical phonons when PZT transition occurs. In fact, there are only two studies which report the calculation of vibrational frequency for  $\text{PbTiO}_3$ . Freire and Katiyar<sup>16</sup> carried out such calculation just by adjusting the parameters of a rigid ion model while Garcia and Vanderbilt<sup>15</sup> performed it using the first-principle calculation. Following the results of these latter authors the tetragonal phase could change either to an orthorhombic or to a monoclinic phase by means of the linear coupling between strain and atomic displacement.

We are reminded of this result because the tetragonal phase in PZT is very similar to that of in  $\text{PbTiO}_3$  and the monoclinic - tetragonal transition is marked by changes in the  $B_1$  symmetry mode. This is very interesting because this mode involves only oxygen motion [ $O_{1z} - O_{2z}$ ] where both oxygen atoms move in opposite directions leading to the tetragonal symmetry-breaking. However, this mode appears to be dependent of the Zr/Ti ratio as demonstrated by Frantti et al<sup>10</sup> whose part of these results are reproduced in Fig. 3b. When the temperature is kept constant, the variable responsible for the transition is the Zr/Ti ratio. It is well-known that the tetragonal strain,  $c_t/a_t$ , decreases when Zr content increases. Taking into account this fact, the unit cell can only be distorted by an in-plane strain. Considering that the strain can transform according to the irreducible representation of  $C_{4v}^1$  space group, where the  $E$  distortion leads to a monoclinic symmetry and  $B_1$  and  $B_2$  to an orthorhombic one with axes parallel ( $B_1$ ) or rotated about  $45^\circ$  ( $B_2$ ) with respect to the tetragonal base. In this way, a  $B_2$  distortion should be the transition mechanism since the actual monoclinic phase is just characterized by a rotation of  $45^\circ$  in tetragonal plane. Also, the monoclinic phase can be seen as a pseudo-orthorhombic one due to the very small monoclinic angle  $90^\circ - \beta$  whose origin can be in the delicate balance between temperature- and concentration-induced strain. The lattice dynamical study made by Garcia et al<sup>15</sup> is limited to the edge of the PZT phase diagram where the doubling of the unit cell was not considered. Finally, the observed behavior of optical phonons as a function of concentration seems to be confirmed by means of first-principle calculation considering the effects of Zr/Ti ratio. This can provide a better understanding of the phonon related phase transition in PZT as well as other perovskite systems with similar MPB.

## IV. CONCLUSIONS

In summary, the behavior of the optical modes for  $\text{PbZr}_{1-x}\text{Ti}_x\text{O}_3$  with  $x$  varying from  $x=0.40$  to  $x=0.60$  were reported and discussed. The observed changes were attributed to the phase transitions. At 7 K, we were able to observe the transitions rhombohedral - monoclinic - tetragonal. Our results are in accordance with those recently reported by Noheda et al.<sup>12</sup> and Frantti et al.<sup>10</sup> which studied the stability of monoclinic phase using high resolution synchrotron X-ray powder diffraction technique. Both transitions we have reported are studied in the view of group theory analysis where some optical phonons in the monoclinic phase were assigned. Very of interest is the behavior of  $B_1$  mode that has an unusual concentration dependence in the vicinity of tetragonal-monoclinic phase transition. Further studies in PZT single crystal with monoclinic phase will be need in order to assign each member of doublet  $A' \oplus A''$ .

**Acknowledgements** – The authors wish to acknowledge Dr. I. Guedes for valuable discussions related to this work. One of us, A. G. Souza Filho wishes to acknowledge the fellowship received from FUNCAP. Financial support from FUNCAP, CNPq, FAPESP and FINEP is gratefully acknowledged.

---

\* Corresponding Author: A. G. Souza, FAX 55 (85) 2889903, E-mail: agsf@fisica.ufc.br

<sup>1</sup> B. Jaffe, W.R. Cook, and H. Jaffe, in *Piezoelectric Ceramic*, Academic Press, New York, 1971.

<sup>2</sup> W. Cao and L. E. Cross, Phys. Rev. B **47**, 4825 (1993); J. F. Meng, R. S. Katiyar, G. T. Zou, and X. H. Wang, phys. stat. sol. (a) **164**, 851 (1997).

<sup>3</sup> M. J. Haun, E. Furman, S.J. Jang, and L.E. Cross, Ferroelectrics **99**, 13 (1989); **99**, 63 (1989); M. J. Haun, E. Furman, H. A. McKinstry, and L. E. Cross, *ibid.* **99**, 27 (1989); M. J. Haun, Z. Q. Zhuang, E. Furman, S. J. Jang, and L. E. Cross, *ibid.* **99**, 45 (1989); M. J. Haun, E. Furman, T. R. Halemane, and L. E. Cross, *ibid.* **99**, 55 (1989).

<sup>4</sup> V. A. Isupov, Soviet Physics-Solid State **10**, 989 (1968); **12**, 1084 (1970); K. Carl and K. H. Harftl. phys. stat. sol.(a) **8**, 87 (1971); L. Bemguigui, Solid State Commun. **11**, 825 (1972); W. Cao and L. E. Cross, J. Appl. Phys. **73**, 3250 (1993)

<sup>5</sup> B. Noheda, D. E. Cox, G. Shirane, J. A. Gonzalo, S.E. Park and L. E. Cross, Appl. Phys. Lett. **74**, 2059 (1999);

<sup>6</sup> B. Noheda, J.A. Gonzalo, L.E. Cross, R. Guo, S-E. Park, D.E. Cox, and G. Shirane, Phys. Rev. B **61**, 8687 (2000); R. Guo, L. E. Cross, S-E.Park, B.Noheda, D.E. Cox, and G. Shirane, Phys. Rev. Letters **87**, 5423 (2000)

<sup>7</sup> D.L. Corker, A.M. Glazer, R.W. Whatmore, A. Stallard, and F. Fauth, J. Phys.:Condens. Matter **10**, 6251 (1998).

<sup>8</sup> L. Bellaiche, A. Garcia, and D. Vanderbilt, Phys. Rev. Lett. **84**, 5427 (2000).

<sup>9</sup> A.G. Souza Filho, K.C.V. Lima, A.P. Ayala, I. Guedes, P.T.C. Freire, J. Mendes Filho, E.B. Araujo, and J. A. Eiras, Phys. Rev. B **61**, 14283 (2000).

<sup>10</sup> J. Frantti, V. Lanto, S. Nishio, and M. Kakihama, Jpn. J. Appl. Phys. **38**, 5679 (1999).

<sup>11</sup> G. Burns and B. A. Scott, Phys. Rev. B **7**, 3088 (1973).

<sup>12</sup> B. Noheda, D. E. Cox, G. Shirane, R. Guo, B. Jones and L. E. Cross, cond-mat/0006752 (unpublished).

<sup>13</sup> A. Amin, R. E. Newnham, L. E. Cross, and D. E. Cox, J. Solid State Chem. **37**, 248 (1981).

<sup>14</sup> I. El-Harrad, P. Becker, C. Carbatos-Ndelec, J. Handerek, Z. Ujma, and D. Dmytrow, J. Appl. Phys. **79**, 5581 (1995).

<sup>15</sup> A. Garcia and D. Vanderbilt, Phys. Rev. B **54**, 3817 (1996).

<sup>16</sup> J. D. Freire and R. S. Katiyar, Phys. Rev. B **37**, 2074 (1998).

FIG. 1. Raman spectra of  $\text{PbZr}_{1-x}\text{Ti}_x\text{O}_3$  ceramics recorded at 7 K. The numbers stand for Ti concentration.

FIG. 2. Raman spectrum of  $\text{PbZr}_{0.40}\text{Ti}_{0.60}\text{O}_3$  illustrating the fitting procedure employed to deconvolute it in a set of Lorentzian curves.

FIG. 3. a) Variation of the frequency of some Raman modes as a function of concentration recorded at 7 K; b) a small frequency region shown in a) is depicted and; c) the splitting  $\Delta\omega$  ( $\omega_{B_1-\omega_E}$  in tetragonal phase and  $\omega_{A''}$ -the highest frequency member of  $A' \oplus A''$  in monoclinic phase. The dotted lines in a) and b) represent the transition region among rhombohedral (R), monoclinic (M), and tetragonal (T). The vertical dotted line in c) is only a guide for eyes. The labels stand for symmetry modes in different phases. The open-circles and open-square are data from Ref.<sup>10</sup> and Ref.<sup>11</sup> where all solid-circles are data from the present work.

FIG. 4. Correlation table for some modes belonging to the monoclinic ( $C_s$ ), tetragonal ( $C_{4v}$ ), and rhombohedral ( $C_{3v}$ ) phase originated from  $T_{2u}$  in cubic ( $O_h$ ) phase.

TABLE I. The values of each member of the doublet showed in Fig. 3b for various compositions of PZT recorded at 7 K. The frequencies are in units of  $\text{cm}^{-1}$ . The label  $a$  and  $b$  stands for results obtained in this work and in Ref.<sup>10</sup>, respectively.

$\text{PbZr}_{1-x}\text{Ti}_x\text{O}_3$	This work	Frantti et al. <sup>10</sup>
$\text{PbZr}_{0.525}\text{Ti}_{0.475}\text{O}_3$	270,287	
$\text{PbZr}_{0.52}\text{Ti}_{0.48}\text{O}_3$	272,294	
$\text{PbZr}_{0.51}\text{Ti}_{0.49}\text{O}_3$		267,293
$\text{PbZr}_{0.50}\text{Ti}_{0.50}\text{O}_3$	268,293	267,293
$\text{PbZr}_{0.49}\text{Ti}_{0.51}\text{O}_3$	267,292	
$\text{PbZr}_{0.48}\text{Ti}_{0.52}\text{O}_3$	268,291	
$\text{PbZr}_{0.45}\text{Ti}_{0.55}\text{O}_3$	267,289	
$\text{PbZr}_{0.42}\text{Ti}_{0.58}\text{O}_3$	271,287	

$\text{PbZr}_{0.40}\text{Ti}_{0.60}\text{O}_3$	272,288	271,286
$\text{PbZr}_{0.30}\text{Ti}_{0.70}\text{O}_3$		277,287
$\text{PbZr}_{0.20}\text{Ti}_{0.80}\text{O}_3$		282,289
$\text{PbZr}_{0.10}\text{Ti}_{0.90}\text{O}_3$		287,291

---

---

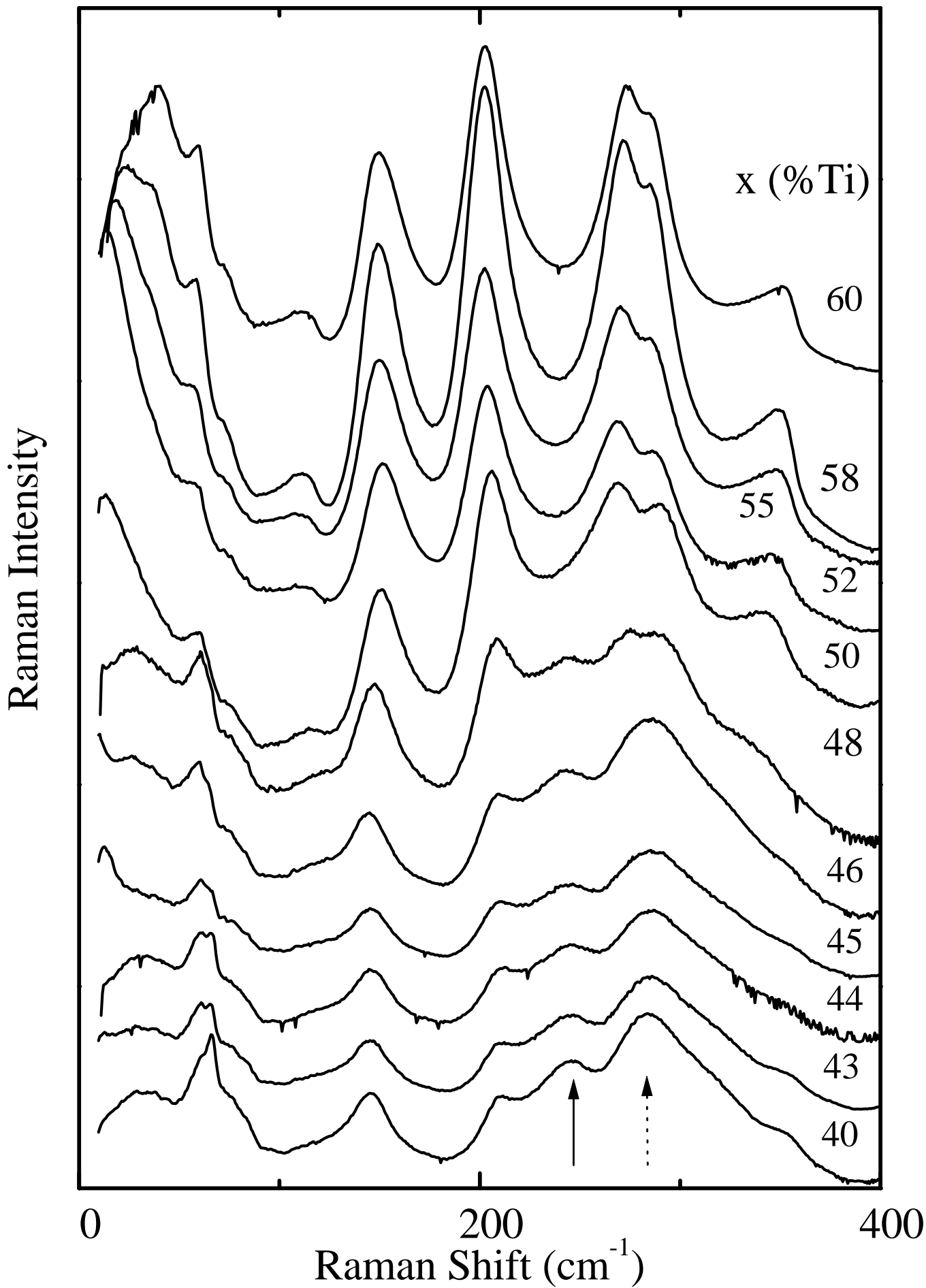
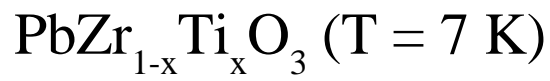


Fig. 1. A. G. Souza et al.

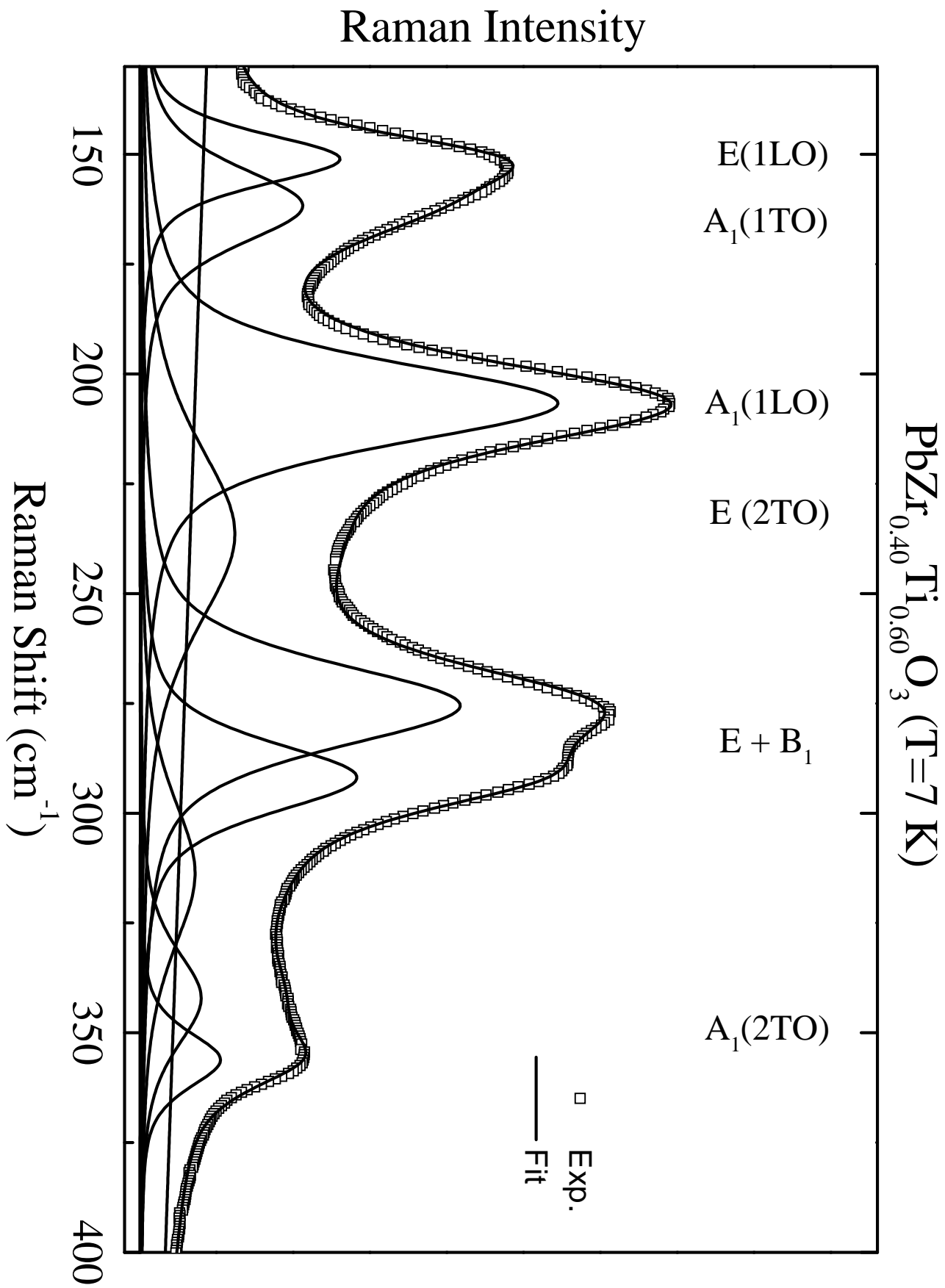


Fig. 2. A.G. Souza et al.

Fig. 3. A. G. Souza et al

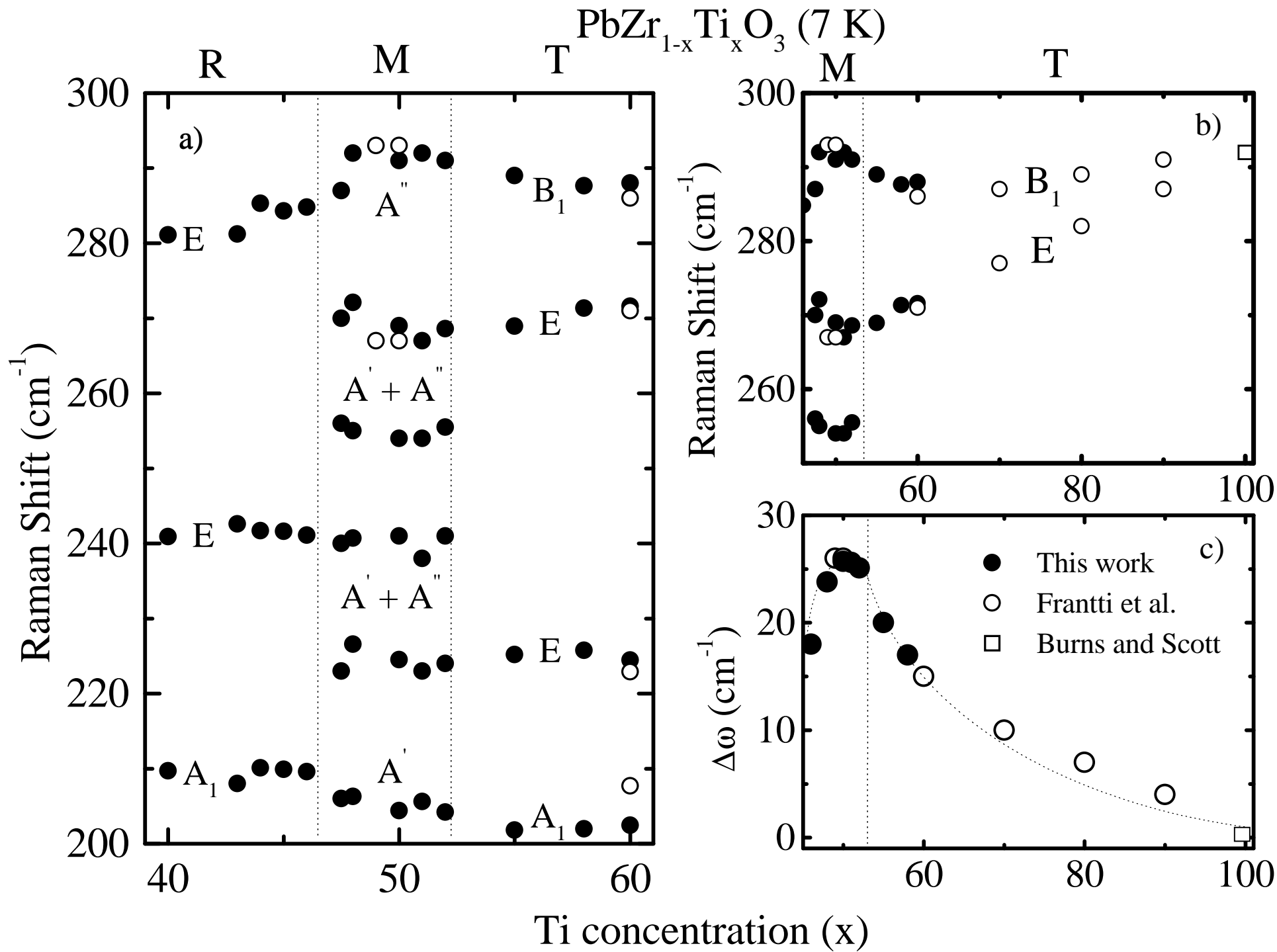




Fig. 4. A.G. Souza et al.

Point Group	$O_h$	$C_{3v}$	$C_s$	$C_{4v}$	$O_h$
Irreducible Representations	$T_{2u}$	$A_2$ $E$	$A'$ $A''$	$B_1$ $E$	$T_{2u}$